ARTICLE

JAAS
www.rsc.org/jaas

Calculation of cathode heating in analytical glow discharges†

Annemie Bogaerts* and Renaat Gijbels

Department of Chemistry, University of Antwerp, Universiteitsplein 1, B-2610 Wilrijk-Antwerp, Belgium. E-mail: annemie.bogaerts@ua.ac.be

Received 12th January 2004, Accepted 20th February 2004
First published as an Advance Article on the web 21st April 2004

The temperature of the cathode (sample) in analytical glow discharges is calculated as a function of depth in the sample, by means of a one-dimensional heat conduction equation. The energy input is determined by the energetic ions and atoms bombarding the cathode. Calculations are performed for a Cu sample, under various conditions, ranging from perfect cooling from the backside, to the limit of no cooling. The effect of the discharge conditions (voltage–pressure–current) is also investigated. Finally, simulations are carried out for various cathode materials. It is found that the efficiency of cooling has a very important effect on the cathode surface temperature. Moreover, different cathode materials can give rise to great differences in the cathode surface temperature for the same power input, due to a different thermal conductivity.

1. Introduction

It is generally known that the cathode of analytical glow discharges can become quite hot, as a result of the bombardment of energetic ions and atoms from the plasma, when no or inappropriate cooling is applied. Mai and Scholze[1] stated that the temperature of compacted Cu powder samples amounted to 800–900 K, at high electrical power. Sanz-Medel and coworkers[2] have shown SEM (Scanning Electron Microscopy) images of painted samples sputtered by rf-GD-OES, which illustrate that, in the case of no cooling, or only cooling from the back of the sample with circulating water at 2 °C, the craters are characterized by morphological and topographical alterations with irregularly distributed bubbles. Since this can give rise to a loss in depth resolution, it was suggested not only to cool the back side of the sample but also the limiting cathode disk.[2]

Cooling in analytical glow discharges is typically carried out with water circulation through a cooling block behind the sample and/or through the cathode plate at the front of the sample[2–5] (*e.g.*, in Grimm-type discharges), or by cryocooling with liquid nitrogen, of either the discharge chamber or the sample.[6–13] However, even in the case of cooling, the cathode temperature can still rise to a large extent, when high electrical power is applied to the glow discharge, or when the cooling is not appropriate (*e.g.*, when there is bad thermal contact between cooling block and sample). Recently, Hieftje and coworkers[14] have estimated that the cathode temperature is between 545 and 600 K, in a glow discharge at 3 Torr and 65 mA, in spite of the fact that cooling of the cathode is applied.[14]

The importance of cooling was stressed by several authors. It seems to have significant effect, both on the plasma processes (*e.g.*, gas temperature, excitation and rotation temperature),[6] on the analytical performance,[7–10,15] and on the glow discharge behaviour in general. For instance, a hot cathode leads to a higher gas temperature, and this affects the current–voltage–pressure characteristics.[16–18]

Gas temperature and cathode temperature are not often measured in analytical glow discharges, but they are both very important from fundamental and analytical point of view (see above). In ref. 17, we have presented a model to calculate the gas temperature, and it was demonstrated that it has a large effect on the current–voltage–pressure characteristics. However, the exact gas temperature was subject to uncertainties, because the calculation result depended very much on the assumed boundary condition, *i.e.*, the temperature at the cathode, and the latter was also unknown. Therefore, in the present paper, we intend to estimate the cathode temperature, based on the one-dimensional heat conduction equation.

Wilken *et al.*[19] have also calculated the sample surface temperature, based on a cylindrically symmetric heat conduction equation, in order to determine the expansion and contraction of the sample surface. They calculated a temperature increase at the surface of up to 100 K, and steady state was reached after a few seconds. They performed calculations for several fixed values of the power input into the sample.[19]

In our model, the power input is calculated explicitly from the bombardment of energetic ions and atoms from the glow discharge plasma. It should, however, be noted that our calculations are also not fully self-consistent, because this energy input is taken from previous calculations, and in reality, the input power will not be fixed (constant in time), but will change when the cathode temperature rises. However, the present assumptions are good enough to illustrate the cathode heating effects.

The calculation method will be described in Section 2. In Section 3, the calculated cathode temperature will be illustrated, and the important effect of cooling will be discussed. The effect of discharge conditions (*i.e.*, electrical power) on the calculated cathode temperature will also be presented, and comparison will also be made for different cathode materials. Finally, conclusions will be given in Section 4.

2. Description of the calculation method

The temperature of the cathode surface, as well as the temperature distribution inside the cathode material, are calculated with the heat conduction equation. As mentioned above, the energy input into the cathode, responsible for the heating, is due to the bombardment of energetic ions and atoms from the glow discharge plasma. We assume here for simplicity that the energy input is uniform in the radial direction, which is in any case required to obtain flat craters, hence for good depth profiling. Therefore, the heat conduction equation is only considered in one dimension:

$$\frac{\partial T(x,t)}{\partial t} = \frac{\partial}{\partial x}\left[\frac{\kappa}{C_{\mathrm{P}}\rho}\left(\frac{\partial T}{\partial x}\right)\right] + \frac{1}{C_{\mathrm{P}}\rho dx}\left[\left(\frac{\partial E}{\partial t}\right)_{\mathrm{input}} - \left(\frac{\partial E}{\partial t}\right)_{\mathrm{loss}}\right]$$

κ, C_{p} and ρ are the thermal conductivity, heat capacity and mass density of the cathode material, respectively. The term at

† Presented at the 2004 Winter Conference on Plasma Spectrochemistry, Fort Lauderdale, FL, USA on January 5–10, 2004.

DOI: 10.1039/b400483c

the left-hand side represents the time-evolution of the temperature. The first term at the right-hand side stands for the spatial variation as a result of heat conduction, whereas the last term at the right-hand side gives the energy input minus the energy loss per time unit, responsible for the temperature evolution.

The energy input term, due to the bombardment of energetic plasma species, *i.e.*, Ar^+ ions, fast Ar atoms, as well as ions of the cathode material (M^+),[20] is calculated as:

$$\left(\frac{\partial E}{\partial t}\right)_{\text{input}} = \int_E f_{Ar^+}(E)\mathrm{d}E * E_{Ar^+} + \int_E f_{Ar^0}(E)\mathrm{d}E * E_{Ar^0} + \int_E f_{M^+}(E)\mathrm{d}E * E_{M^+}$$

where $f(E)$ stands for the flux energy distributions (in $cm^{-2}\,s^{-1}$) of the bombarding species (Ar^+, Ar^0 and M^+). Hence, multiplying these flux energy distributions with the corresponding energy, and integrating over all energies, yields the power input (or energy input per time). As mentioned above, by using a fixed energy input, the calculations are not completely self-consistent. Indeed, in reality, a rise in the cathode temperature will affect the discharge through the gas temperature, and that will slightly change the energy input. However, the approximation of a fixed energy input is good enough here, to illustrate the cathode heating effect.

Since the typical implantation depth in glow discharges is only in the order of a few nm,[21,22] which is much smaller than the spatial grid in the calculation, we assume that this energy input only takes place at the first grid position (*i.e.*, representing the surface).

The energy loss per unit time is in practice due to cooling, but it is not straightforward to predict this cooling as an energy loss term. Therefore, the cooling is taken into account in the model, by using a suitable boundary condition for the temperature. We assume water cooling from the backside, by using a Cu cooling block of 1 cm thickness, with the water flowing in the middle of it. Further, we assume that the water has a temperature of 40 °C (313 K).[23] The sample thickness then determines the distance between the surface and the position at which the cooling is applied. Because the heat transfer between the water and the Cu cooling block is very efficient, in case of perfect contact, it can be assumed that the cooling block has the same temperature as the water, at the position of the water cooling. Therefore, the boundary condition, in case of perfect cooling, is taken as $T = 313$ K, at the distance defined by the thickness of the sample + 0.5 cm (*i.e.*, position of cooling water in the middle of the cooling block).

Another possible loss mechanism, which only comes into play at very high surface temperature (*e.g.*, in case of no cooling at all), is given by the energy loss due to evaporation of the sample material. Indeed, in this extreme situation, when the temperature of the sample exceeds the melting point, the material would start melting, and when the temperature rises further and exceeds the boiling point, it could even start evaporating. Although not important in most of the practical glow discharge situations, the mechanisms of melting and vaporization are taken into account in the model. When the cathode temperature at a certain distance from the surface would reach the melting point, the temperature at this position stays constant with further energy input, during the phase transition. With still more energy input, the further temperature rise can again be calculated with the above heat conduction equation, but using thermal properties of liquid material.

When the temperature would rise further, vaporization could start playing a role, and consequently, this has to be taken into account as energy loss mechanism in the heat conduction equation. This energy loss is calculated from the mole flux of evaporated atoms, multiplied with the molar heat of vaporization. The mole flux of evaporated atoms, j_{evap}, is determined from the vapour pressure at the surface temperature, $p_{\text{vap}}(T_s)$, which is calculated by integrating Clausius–Clapeyron equation:

$$p_{\text{vap}}(T_s) = p_0 \exp\left[-\frac{\Delta H_{\text{lv}}}{R}\left(\frac{1}{T_s} - \frac{1}{T_b}\right)\right]$$

$$j_{\text{evap}}(T_s) = \frac{A p_{\text{vap}}(T_s)}{\sqrt{2\pi M R T_s}}$$

Here, T_s and T_b represent the surface temperature and the normal boiling temperature at pressure $p_0 = 1$ atm. ΔH_{lv} is the heat of vaporization (*i.e.*, transition from liquid to vapour), R is the gas constant, M is the molecular mass of the evaporated atoms, and A represents a sticking coefficient, which is usually taken equal to unity for metals. However, because the power input in glow discharge sputtering is typically quite low (see further), this loss mechanism is in practice negligible in the present case, except when the target is not cooled efficiently, and the target temperature would become very high (see below).

The one-dimensional heat conduction equation is calculated with an explicit finite difference method, and yields the temperature distribution inside the cathode (sample) as a function of time.

3. Results and discussion

The calculations will be performed for a Grimm-type glow discharge cell, at typical conditions used for GD-OES, *i.e.*, pressure between 440 and 1200 Pa, a discharge voltage between 800 and 1200 V, and an electrical current of 6–50 mA.[24] Indeed, the Grimm-type source typically operates at higher electrical power than, for instance, the VG9000 glow discharge cell used for GDMS, and hence the cathode heating will be more pronounced. The energy input due to the bombardment of Ar^+ ions, fast Ar atoms and Cu^+ ions is adopted from our previous modeling work for these conditions.[24] In first instance, we will focus on Cu as the cathode material, and we will investigate the influence of cooling efficiency. Moreover, we will also study the effect of operating conditions (voltage, pressure, current) on the cathode heating. Afterwards, the cathode temperature will be calculated for different cathode materials, and the consequences for practical glow discharge analysis will be discussed.

3.1. Cu sample: Effect of cooling efficiency

As mentioned above, the effect of cooling is taken into account in the model, by assuming as the boundary condition a temperature of 313 K at a certain distance, defined by the sample thickness + 0.5 cm (*i.e.*, halfway the Cu cooling block of 1 cm). In first instance, we assume perfect contact between the sample and the cooling block.

Fig. 1 shows the calculated temperature distribution in a sample of 1 cm thickness, as a function of time, for a gas pressure of 850 Pa, a discharge voltage of 800 V, and an electrical current of 25 mA. For these conditions, the input power as a result of bombardment of the energetic plasma species was calculated to be 70.3 W cm^{-2}, which means 8.8 W for an anode diameter of 4 mm. Hence, this corresponds to 44% of the electrical power (which is equal to 20 W).

In the beginning, the sample temperature is 300 K, which was set as initial condition. As time evolves, the temperature at the surface rises, due to the bombardment of energetic species. As a result of heat conduction, the temperature inside the cathode material rises as well. However, due to the boundary condition ($T = 313$ K) at a depth of 1.5 cm (*i.e.*, thickness of the sample

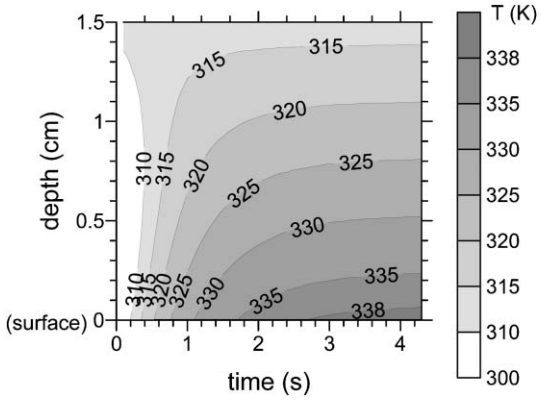

Fig. 1 Calculated temperature profile inside the cathode material, as a function of time, for a Cu sample of 1 cm thickness, at 850 Pa, 800 V and 25 mA. The surface is found at depth = 0 cm, and the cooling (represented by a boundary condition: $T = 313$ K) takes place at a depth of 1.5 cm (= sample thickness + 0.5 cm of cooling block).

+ 0.5 cm), the temperature rise is limited to about 339 K at the maximum (*i.e.*, at the surface). After about 4 s, the sample temperature appears to have reached steady state, and the temperature will remain constant in time, as long as the cathode bombardment and sample cooling remain the same. These results are in fairly good agreement with the data presented by Wilken *et al.*,[19] when taking into account the differences in power input, kind of material and boundary conditions.

It should be mentioned that this calculated time-evolution is not completely self-consistent, because the energy input was fixed (constant in time). In reality, the rise in cathode temperature yields a change in the plasma behaviour, through a change in gas temperature, and hence the energy input will also change slightly as a function of time. It is, however, expected that this effect has no major influence on the calculated time-evolution of the cathode temperature.

The effect of sample thickness on the temperature is shown in Fig. 2. A thicker sample means that the cooling takes place further away from the surface. From Fig. 2a, it is clear that the temperature profile in the sample is the same in all cases, *i.e.*, characterized by a linear gradient. Consequently, the surface temperature is higher for the thicker samples. As shown in Fig. 2b, it also takes a longer time before steady state is reached for the thicker samples. However, in all these cases, the surface temperature is still quite low (*i.e.*, less than 100 °C). It is clear that these values represent the lower limit, when the cooling is very efficient.

When the cooling is not perfect, *i.e.*, when there is no good thermal contact between cooling block and sample, the heat conductivity at the contact position will be much lower than the bulk value of Cu. However, it depends on how bad the contact is, and the latter is generally not known exactly. Hence, this effect cannot easily be described in the heat conduction equation. Moreover, bad thermal contact will probably be a two-dimensional (or even three-dimensional) effect, which can, therefore, not be described with our one-dimensional model. Therefore, in order to represent the effect of inefficient cooling, we have assumed as the boundary condition different temperature values at the end of the Cu sample (*i.e.*, contact position with the cooling block), and the result is shown in Fig. 3, for a sample thickness of 1 cm. The thick solid line represents the case of perfect contact, and a boundary condition of $T = 313$ K at 1.5 cm. The other curves are the result of imperfect contact, illustrated by a temperature jump at the contact position (1 cm depth). As mentioned above, the exact value of the temperature jump is not known, hence we have simulated a few cases, with a temperature jump at the contact position (1 cm depth) of 30 K, 80 K, 130 K and 180 K.

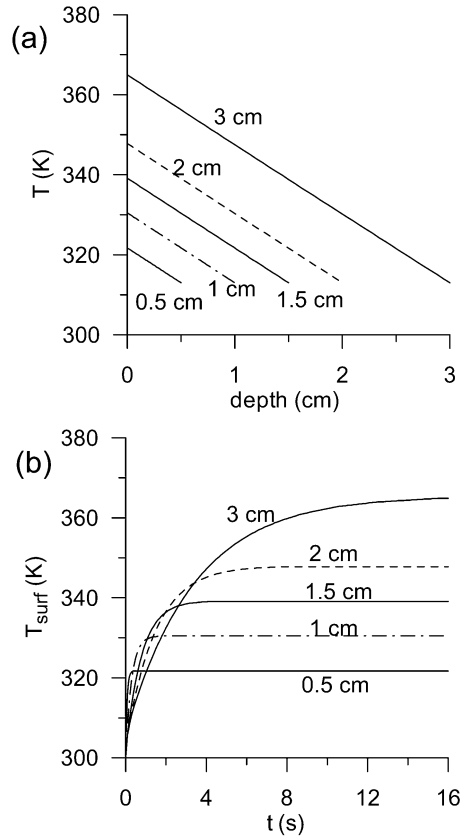

Fig. 2 Calculated temperature profiles inside the cathode material at steady state (a) and calculated cathode surface temperature as a function of time (b), for a Cu sample with varying thicknesses, at 850 Pa, 800 V and 25 mA. The various curves are labelled according to the position of cooling, which is at a depth equal to the sample thickness + 0.5 cm (*i.e.*, halfway point of the cooling block of 1 cm). The cooling is represented by the boundary condition: $T = 313$ K.

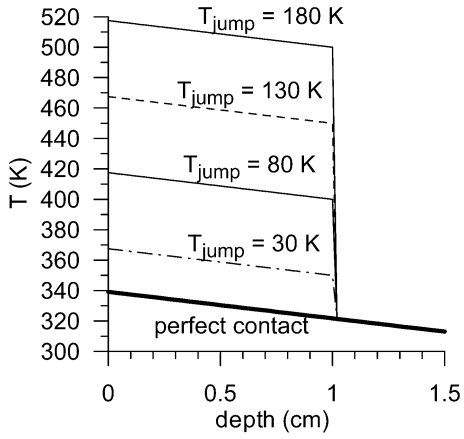

Fig. 3 Calculated temperature profiles inside the cathode material at steady state, for a Cu sample of 1 cm thickness, at 850 Pa, 800 V and 25 mA. The thick solid line stands for perfect cooling. The other lines represent several degrees of imperfect contact between cooling block and Cu sample, indicated by the temperature jumps at the end of the sample (*i.e.*, at a depth of 1 cm).

It appears from Fig. 3 that the temperature gradients inside the Cu cathode material itself are all linear, with the same slope, independent from the value of the boundary condition. Indeed, the slope depends only on the material thermal conductivity, and on the power input value, which are the same for all curves in Fig. 3. The value of the boundary condition only determines the absolute value of the surface temperature. In other words, the surface temperature rises linearly with increasing temperature value at the boundary. This explicitly indicates that the

cathode surface temperature depends strongly on the efficiency of cooling.

Finally, as an upper limit for the temperature in the case of inefficient cooling (or in other words: the absence of cooling), we have applied the heat conduction equation with another kind of boundary condition, *i.e.*, $T = T_{\text{initial}}$ (= 300 K) for infinite distance ($x \rightarrow \infty$).

It is clear that in this case, the surface temperature would rise to very high values (*i.e.*, more than 1000 K), as appears from Fig. 4. Note that the sample thickness is here undefined, because the result is independent from this value. In fact, these calculations were performed for "infinitely" thick samples (see boundary condition above).

It appears from Fig. 4 that steady state is only reached after about 3000 s, or almost 1 h. Such a steady increase in surface temperature as a function of time is also experimentally observed in case of no or bad cooling.[23] Note that for short sputtering times, the cathode heating is, however, still limited, but of course, steady state is then not yet reached.

Again, as mentioned above, this calculated time-evolution is not completely self-consistent, because the energy input is taken constant in time, and in reality, it will change as a function of time, because the rise in cathode temperature yields a change in discharge conditions, and hence a change in energy input, due to the bombardment of plasma species. In contrast to our previous calculations, where efficient cooling was applied, and the temperature rise was not so high, the assumption of a constant energy input is here a somewhat stronger approximation.

Fig. 5a illustrates the calculated temperature profile within the sample as a function of time, in the case without cooling. Because of the high surface temperature, and the good thermal conductivity of Cu, the temperature inside the cathode material increases also to very high values, even very deep in the material, *i.e.*, much deeper than the thickness of real samples. Therefore, this figure does not represent a real glow discharge case, but it is useful as an illustration, to obtain a better feeling about the heat conduction inside a Cu sample. It is clear from this figure that, in the case without cooling, the temperature at the back of the sample would be very high, even for not too long analysis times. For instance, at 1000 s (*i.e.*, about 17 min), the temperature at the surface is calculated to be about 1200 K, and the temperature at the back of a sample of a few cm thickness is only a few tens of K less, as appears also from the slopes of the curves in Fig. 3.

At these high temperature values, melting and even vaporization of the cathode material could start playing a role in glow discharges. Fig. 5b illustrates the calculated fraction of molten sample material as a function of time and depth in the material (1 = 100% molten, 0 = 100% solid, and between 0 and 1 indicates partially molten). The material starts melting when

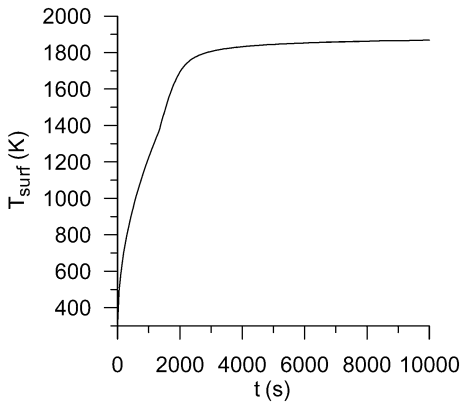

Fig. 4 Calculated cathode surface temperature as a function of time, for a Cu sample at 850 Pa, 800 V and 25 mA, in the case without cooling.

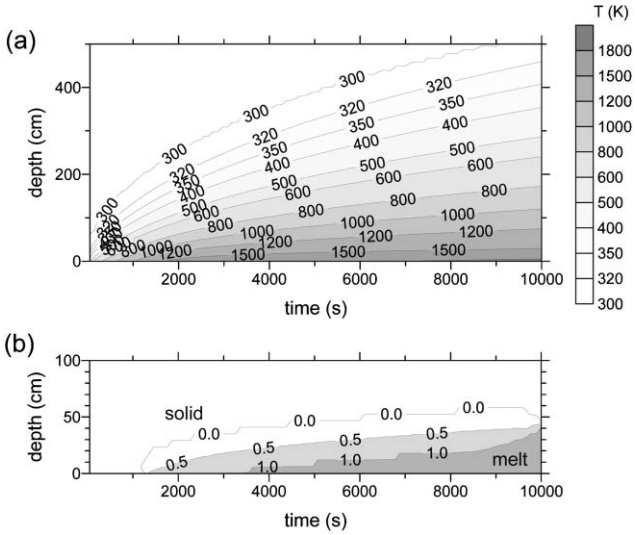

Fig. 5 Calculated temperature profile inside the cathode material (a), as a function of time, for Cu, at 850 Pa, 800 V and 25 mA, in case that no cooling is applied. Also shown is the fraction of molten material as a function of time and depth, for the same conditions as in (a), (fraction 1 means 100% molten; fraction 0 means 100% solid; fraction between 0 and 1 stands for partially molten material).

the temperature exceeds the melting point of Cu (*i.e.*, 1358 K), and the fraction of molten material increases as a function of time. Again, this figure is not very realistic for practical analysis times and sample thicknesses, but it is informative as an illustration. For instance, it is clear from this figure that after about 1 h of analysis time, a Cu sample (with typical thickness of a few cm) would be entirely molten, in case of no cooling.

Beside melting, the material would also start to evaporate after about 1300 s (or 22 min), in case of no cooling. Fig. 6 shows the flux of evaporated atoms as a function of time (solid line), in comparison with the flux of sputtered atoms (dashed line). Again, the sample thickness is undefined here, because of the applied boundary condition ($T = T_{\text{initial}}$ for $x \rightarrow \infty$; see above).

Whereas the flux of sputtered atoms is calculated to be about 1.7×10^{18} cm^{-2} s^{-1} (constant as a function of time), the flux of evaporated atoms increases as a function of time. At about 1600 s (or 27 min), the flux of evaporated atoms is comparable to the flux of sputtered atoms, but at longer times, the evaporation flux becomes much higher. Hence, in this (theoretical) limit of no cooling, evaporation could be the dominant sample-atomization mechanism.

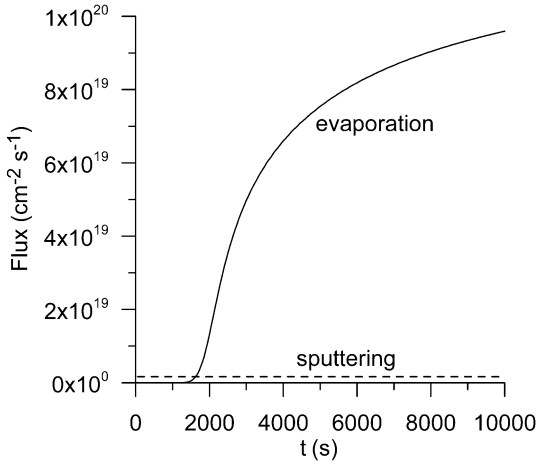

Fig. 6 Calculated flux of evaporated atoms (solid line) and sputtered atoms (dashed line) as a function of time, for a Cu sample, at 850 Pa, 800 V and 25 mA, in the case of no cooling.

Hagelaar and Pitchford have theoretically investigated the importance of evaporation of Zn cathodes in GD-OES.[25] They found that for Zn, which has a high vapour pressure in the solid phase, evaporation is even important below the melting point. In our model, we assume that, upon increase of temperature, first melting occurs, and only for higher temperatures evaporation starts playing a role. This is true for most metals (such as Cu), which have a much lower vapour pressure in the solid phase. Hence, even for these materials, it seems that evaporation (from the liquid phase) can play a role, but of course only in the extreme case of no (or very bad) cooling.

Of course, to summarize, the above results for the upper limit of no cooling, are only by way of illustration, because a glow discharge will never be operated for such a long time without cooling. The real temperature inside the cathode material will be somewhere in between the limits of perfect cooling and no cooling. The results, however, clearly demonstrate that the cooling efficiency has obviously a major effect on the cathode temperature. Moreover, since this parameter determines the gas temperature, and hence the electrical and also analytical conditions, attention should be paid to the cooling efficiency, as was also pointed out in ref. 16.

3.2. Cu sample: Effect of discharge conditions

It is clear that the cathode surface temperature will increase more for higher energy input from the bombarding plasma species, and the latter will be higher for higher values of voltage and current. Fig. 7 shows the calculated temperature distribution inside a Cu sample of 1 cm thickness (*i.e.*, cooling at 1.5 cm, with boundary condition $T = 313$ K), after steady state is reached, for various conditions of pressure, voltage and current. The value of the power input into the cathode material, due to the bombardment of energetic plasma species, is also given for each curve. We found that this power input is always around 45% of the electrical power. Hence, a rise in voltage and current results in an increase in the input power into the cathode, and consequently in a higher cathode temperature, as is clear from Fig. 7. However, in this case of perfect cooling, the surface temperature never exceeded 400 K, even for the highest voltage and current investigated (1000 V, 50 mA). This indicates that the discharge conditions have some effect on the cathode temperature, but for the typical operating conditions of analytical glow discharges, the effect is of minor importance, compared to the efficiency of cooling.

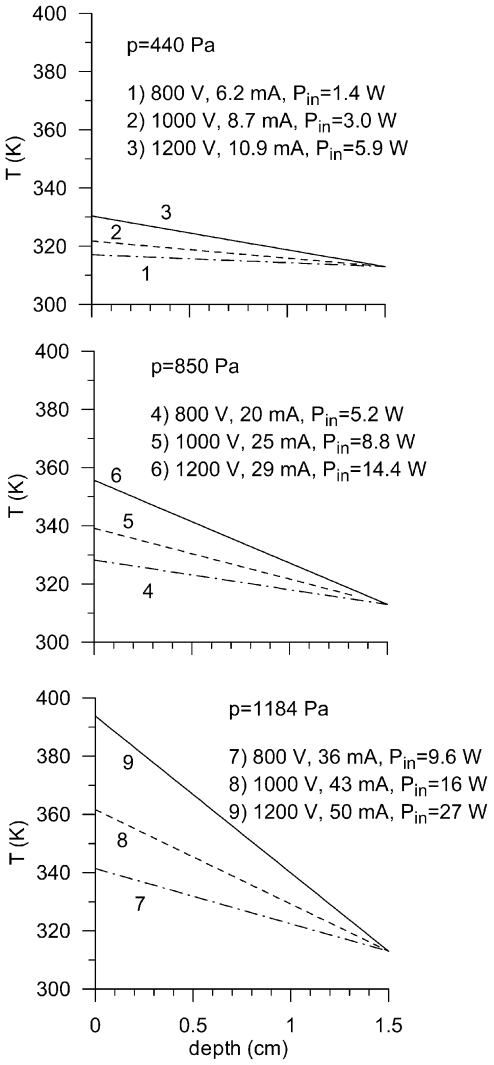

Fig. 7 Calculated temperature profiles inside the cathode material at steady state, for a Cu sample of 1 cm thickness, in case of perfect cooling (boundary condition: $T = 313$ K at a depth of 1.5 cm), for various conditions of pressure, voltage and current. For every curve, the power input into the sample due to bombardment of energetic plasma species is also indicated (P_{in}).

3.3. Effect of sample material

Finally, we have performed calculations for various cathode materials, with different thermal properties. The input data for the different materials were adopted from ref. 26. Again, the calculations are not fully self-consistent, because the energy input due to the bombardment of energetic plasma species was taken from our previous calculations for Cu, and the fact that a different material yielded a different cathode temperature, and hence somewhat different plasma conditions, is not taken into account in this cathode heating source term. However, this effect is not so large, so it will not have much effect on our calculation results. The different thermal properties of the different materials have a much larger effect, and that is correctly taken into account in the model.

Fig. 8a illustrates the calculated temperature profiles at steady state conditions, for various materials. The sample thickness (1 cm) and the boundary conditions ($T = 313$ K at 1.5 cm depth) are taken as constant, as well as the operating conditions (*i.e.*, input power into the cathode material of 8.83 W, see above). It is clear that big differences exist between the calculated cathode temperatures of different materials, which are directly related to the thermal conductivity. Cu has a very high thermal conductivity ($\kappa = 401$ W m^{-1} K^{-1}),[26] which results in a rather low surface temperature (*ca.* 340 K, for the conditions under study here), because the heat is easily conducted towards the inside of the material, and the boundary condition at 1.5 cm depth has significant impact on the rest of the cathode. Zn and Fe have a somewhat lower thermal conductivity (*i.e.*, $\kappa = 116$ and 80 W m^{-1} K^{-1}, respectively[26]), and therefore, the cathode surface temperature can rise to somewhat higher values, for the same conditions (*i.e.*, *ca.* 380 K and 410 K, respectively). Ti, alumina (Al_2O_3) and stainless steel are characterized by still lower thermal conductivities (*i.e.*, $\kappa =$ 22, 17 and 15 W m^{-1} K^{-1}, respectively[26]), and this is reflected in clearly higher cathode surface temperatures, as follows from Fig. 8a. Note that the temperature gradient between 1 and 1.5 cm depth is the same for all curves, because this relates to the Cu cooling block.

For these materials, not only is the cathode surface temperature at steady state conditions higher, but it also takes a longer time before steady state is reached, as is illustrated in Fig. 8b. Whereas for Cu, the time to reach steady state is only a few seconds, it takes in the order of 1 min for stainless steel. It should be mentioned that not only the thermal conductivity (κ), but also the specific heat (C_p) and the mass density (ρ) of the materials play a role in determining when steady state is reached (see heat conduction equation, above).

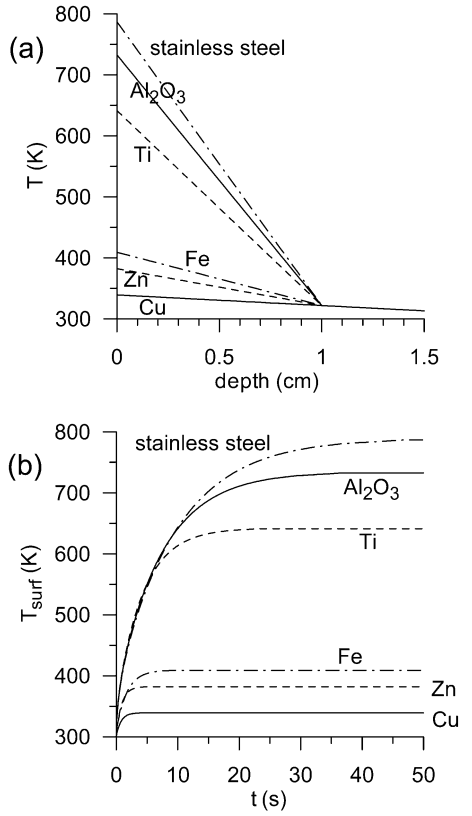

Fig. 8 Calculated temperature profiles inside the cathode at steady state (a) and calculated cathode surface temperature as a function of time (b), for various cathode materials of 1 cm thickness, at 850 Pa, 800 V and 25 mA, in the case of perfect cooling (boundary condition: $T = 313$ K at a depth of 1.5 cm). Note that the last 0.5 cm in (a) represents half of the Cu cooling block.

Note that these results are all obtained in the case of perfect cooling, with $T = 313$ K at a depth of 1.5 cm. It is clear that when the cooling is not so efficient, the cathode surface temperature for the different materials will be higher, but the trends will remain the same (since the slope of the curves is only determined by the power input and the thermal conductivity of the material). Hence, it is clear that the cathode surface temperature can show large variations (*i.e.*, several hundreds of K) for different cathode materials, for the same power input and efficiency of cooling.

Experimentally it is well known that different cathode materials can give rise to different electrical characteristics (voltage–pressure–current relations), and this variation cannot solely be explained by differences in the secondary electron emission coefficients.[27] However, since the voltage–pressure–current relations depend strongly on the gas temperature, and the latter is directly related to the cathode surface temperature, the variation in cathode surface temperature, as shown in Fig. 8, can explain why different cathode materials exhibit different electrical characteristics.

This is an important consequence of the cathode heating effect, because it could also be the reason for so-called matrix effects in glow discharge spectrometry, *i.e.*, the different analytical sensitivity of elements for different matrices. Indeed, when a certain matrix (cathode material) yields a higher cathode temperature, and hence gas temperature, and therefore a lower electrical current for the same voltage and pressure (or a higher pressure for the same current and voltage), the elements within that matrix might be less (or more) efficiently ionized or excited, affecting their analytical sensitivity. In practice, however, the influence will probably still be more complicated, because also the secondary electron emission yield plays a role. But in general it seems favourable for good analytical practice, to efficiently cool the sample material, not only to reduce the effect of gaseous impurities (*e.g.*, H_2O vapour), but also to minimize the differences in electrical conditions for different matrices.

Conclusion

We have calculated the temperature distribution inside the cathode material of analytical glow discharges, by means of a one-dimensional heat conduction equation. The cathode is bombarded by energetic plasma species, and this results in a rise in the cathode temperature. It is found that for perfect cooling, the cathode surface temperature, in case of Cu, does not increase to a large extent. However, the efficiency of cooling appears to have a major effect on the cathode surface temperature, and for inappropriate cooling, the cathode surface can become very high. As an illustration, we have also performed calculations for the limit of no cooling. In this case, the cathode surface temperature rises to values above 1000 K, and it takes a long time before the temperature reaches a steady state. Also melting and vaporization can then come into play, when the analysis time would be long enough.

The effect of glow discharge operating conditions on the cathode temperature is also investigated. As expected, a higher pressure, voltage and current yield more energy input into the cathode, which results in a higher cathode temperature. However, the effect is found to be of minor importance, compared to the efficiency of cooling.

Finally, calculations are performed for different cathode materials, and major variations in the cathode surface temperature were obtained, due to differences in the thermal conductivity of the materials. Since the cathode surface temperature determines the gas temperature, and hence the current–voltage–pressure relations, this can explain why different cathode materials exhibit different electrical characteristics.

Acknowledgements

A. Bogaerts is indebted to the Flemish Fund for Scientific Research (FWO) for financial support. The authors also acknowledge financial support from the Federal Services for Scientific, Technical and Cultural Affairs (DWTC/SSTC) of the Prime Minister's Office through IUAP-V. Finally, A. Bogaerts would like to thank V. Hoffmann, A. Bengtson, K. Marshall and C. Xhoffer for the interesting discussions.

References

1 H. Mai and H. Scholze, *Spectrochim. Acta, Part B*, 1986, **41**, 797.
2 M. Fernandez, N. Bordel, R. Pereiro and A. Sanz-Medel, *J. Anal. At. Spectrom.*, 1997, **12**, 1209.
3 C. Beyer, I. Feldmann, D. Gilmour, V. Hoffmann and N. Jakubowski, *Spectrochim. Acta, Part B*, 2002, **57**, 1521.
4 N. P. Ferreira, H. G. C. Human and L. R. P. Butler, *Spectrochim. Acta, Part B*, 1980, **35**, 287.
5 V. Hoffmann, H.-J. Uhlemann, F. Präßler, K. Wetzig and D. Birus, *Fresenius' J. Anal. Chem.*, 1996, **355**, 826.
6 S. K. Ohorodnik and W. W. Harrison, *J. Anal. At. Spectrom.*, 1994, **9**, 991.
7 S. K. Ohorodnik, S. De Gendt, S. L. Tong and W. W. Harrison, *J. Anal. At. Spectrom.*, 1993, **8**, 859.
8 S. De Gendt, R. E. Van Grieken, S. K. Ohorodnik and W. W. Harrison, *Anal. Chem.*, 1995, **67**, 1026.
9 S. De Gendt, W. Schelles, R. Van Grieken and V. Müller, *J. Anal. At. Spectrom.*, 1995, **10**, 681.
10 M. van Straaten, K. Swenters, R. Gijbels, J. Verlinden and E. Adriaenssens, *J. Anal. At. Spectrom.*, 1994, **9**, 1389.
11 S. De Gendt, R. Van Grieken, W. Hang and W. W. Harrison, *J. Anal. At. Spectrom.*, 1995, **10**, 689.
12 A. I. Saprykin, F.-G. Melchers, J. S. Becker and H.-J. Dietze, *Fresenius' J. Anal. Chem.*, 1995, **353**, 570.
13 T. E. Gibeau, M. L. Hartenstein and R. K. Marcus, *J. Am. Soc. Mass Spectrom.*, 1997, **8**, 1214.

14 G. Gamez, A. Bogaerts, F. Andrade and G. M. Hieftje, *Spectrochim. Acta, Part B*; DOI: 10.1096/j.sub. 2003, 12, 002.
15 R. Payling, D. G. Jones and A. Bengtson, *Glow Discharge Optical Emission Spectrometry*, Wiley, Chichester, 1997, ch. 7.5 and 9.1.
16 M. Kasik, C. Michellon and L. C. Pitchford, *J. Anal. At. Spectrom.*, 2002, **17**, 1398.
17 A. Bogaerts, R. Gijbels and V. V. Serikov, *J. Appl. Phys.*, 2000, **87**, 8334.
18 I. Revel, L. C. Pitchford and J. P. Boeuf, *J. Appl. Phys.*, 2000, **88**, 2234.
19 L. Wilken, V. Hoffmann and K. Wetzig, *J. Anal. At. Spectrom.*, 2003, **18**, 1133.
20 A. Bogaerts and R. Gijbels, *J. Appl. Phys.*, 1996, **79**, 1279.
21 K. Shimizu, H. Habazaki, P. Skeldon, G. E. Thompson and G. C. Wood, *Surf. Interface Anal.*, 1999, **27**, 950.
22 A. Bogaerts, Z. Chen and R. Gijbels, *Surf. Interface Anal.*, 2003, **35**, 593.
23 V. Hoffmann, private communication.
24 A. Bogaerts, L. Wilken, V. Hoffmann, R. Gijbels and K. Wetzig, *Spectrochim. Acta, Part B*, 2001, **56**, 551.
25 G. J. M. Hagelaar and L. C. Pitchford, *J. Anal. At. Spectrom.*, 2002, **17**, 1408.
26 D. R. Lide, *CRC Handbook of Chemistry and Physics*, CRC Press, Boca Raton, 83rd edn., 2002–2003.
27 A. Bengtson, private communication.